Journal of Oleo Science
Copyright ©2013 by Japan Oil Chemists' Society
J. Oleo Sci. 62, (5) 271-281 (2013)

JOURNAL OF OLEO SCIENCE
JOS

Monolayer Compression Induces Fluidization in Binary System of Partially Fluorinated Alcohol (*F4H11OH*) with DPPC

Hiromichi Nakahara, Aya Ohmine, Shoko Kai and Osamu Shibata*

Department of Biophysical Chemistry, Faculty of Pharmaceutical Sciences, Nagasaki International University; 2825-7 Huis Ten Bosch, Sasebo, Nagasaki 859-3298, Japan

Abstract: A two-component Langmuir monolayer consisting of (perfluorobutyl)undecanol (*F4H11OH*) and dipalmitoylphosphatidylcholine (DPPC), a major component of pulmonary surfactants in mammals, has been investigated at the air-water interface. The binary monolayer has been systematically examined from both thermodynamic and morphological perspectives. The excess Gibbs free energy of mixing has been calculated from surface pressure (π)–molecular area (A) isotherms, and the results indicate that the miscibility of the two-component system shows a maximum in thermodynamical stability when the mole fraction ($X_{F4H11OH}$) is 0.3. Results from a two-dimensional phase diagram (π vs. $X_{F4H11OH}$) are consistent with these findings and depict the degree of miscibility resulting from the variation in the transition and collapse pressures relative to the concentration of $X_{F4H11OH}$. The miscibility is also supported by *in situ* Brewster angle microscopy and fluorescence microscopy, as well as *ex situ* atomic force microscopy for the system after transfer onto a mica substrate. Aside from temperature, a known driving force for the fluidization of DPPC monolayers is a change in surface composition caused by the addition of additive molecules. In the present study, however, the fluidization is driven by increasing surface pressures even at constant $X_{F4H11OH}$. Such a fluidization is a fascinating property when looked at in context of its potential implications for pulmonary replacement therapy, and hence, this study provides a fundamental insight into designing fluorinated materials for biomedical use.

Key words: Langmuir monolayer, Lung surfactant, DPPC, Fluorinated amphiphile, Surface pressure, Surface potential

1 INTRODUCTION

A partially fluorinated amphiphile possesses a perfluoroalkyl chain (*F*-chain), hydrocarbon chain (*H*-chain), and hydrophilic headgroup. Incorporation of an *F*-chain into typical *H*-chain amphiphiles is expected to endow the resulting amphiphile with the specific characteristics of the *F*-chain. The attributes of *F*-chains include a combination of high gas-dissolving capacity, chemical and biological inertness, low surface tension, and high fluidity[1, 2]. Thus, partially fluorinated amphiphiles have been of great interest and have resulted in numerous studies involving their potential medical applications, particularly with regard to diagnosis and therapy[2-4]. Highly fluorinated compounds have a tendency to accumulate in the environment and in the human body[5-8]. A detailed description of the interfacial behavior and interaction of perfluorocarboxylic acid with dipalmitoylphosphatidylcholine (DPPC), which is a major component in pulmonary surfactants, can be found in a previously published review article[9]. Perfluorooctyl bromide (PFOB, $n_F = 8$) has been investigated for its potential use in oxygen delivery and has exhibited short organ retention times[10, 11]. The amphiphiles with short *F*-chains ($n_F \leq 8$) appear acceptable for use in the clinical field. Indeed, partially fluorinated alcohols of $CF_3(CF_2)_7(CH_2)_m$ OH ($m = 5$ and 11) have been evaluated and found to be advantageous for improving the effectiveness of pulmonary surfactants[12]. Moreover, the interfacial properties of similar alcohols have been reported previously[13]. However, there are very few reports on the mechanisms of interaction between partially fluorinated compounds and biomembrane components[8, 14]. In particular, there are fewer reports on the biophysical interplay incorporated by the shorter *F*-chains ($n_F \leq 6$).

The incorporation of *F*-chains ($n_F \leq 6$) are expected to

*Correspondence to: Osamu Shibata, Department of Biophysical Chemistry, Faculty of Pharmaceutical Sciences, Nagasaki International University; 2825-7 Huis Ten Bosch, Sasebo, Nagasaki 859-3298, Japan
E-mail: wosamu@niu.ac.jp
Accepted January 9, 2013 (received for review December 19, 2012)
Journal of Oleo Science ISSN 1345-8957 print / ISSN 1347-3352 online
http://www.jstage.jst.go.jp/browse/jos/ http://mc.manusriptcentral.com/jjocs

result in a reduction of the organ retention period relative to similar compounds with longer *F*-chains. In addition, the partially fluorinated amphiphiles ($n_F \leq 6$) show irregular and unexpected physicochemical properties[15]. For example, the melting point of the partially fluorinated alcohols ($n_F \leq 6$) is lower than the corresponding hydrogenated and perfluorinated alcohols. Partially fluorinated compounds have a CH_2-CF_2 linkage, which results in a repulsive interactions of the dipoles[16-18]. In addition, *F*-chains execute a corn-swing motion at the fulcrum in the linkage. Both the repulsive interaction and the motion at the linkage are considered to introduce the unique properties of partially fluorinated amphiphiles.

Herein, the authors employ two-dimensional (2-D) monolayers at the air-water interface in order to provide a model for biomembranes and specifically to model the gas exchange surface of the pulmonary alveoli. The 2-D lipid monolayer technique provides a better understanding of the miscibility, interactions, and phase behavior occurring in binary mixtures containing biomembrane components and synthetic amphiphiles[19-22]. In the present study, we utilize (perfluorobutyl) undecanol (*F4H*11OH) as the partially fluorinated amphiphile. The interfacial interaction of *F4H*11OH with DPPC in the monolayer state has been evaluated by surface pressure (π)-molecular area (*A*) and surface potential (ΔV)-*A* isotherms on 0.15 M NaCl at 298.2 K. The excess Gibbs free energy of binary mixing and an interaction parameter for the binary monolayer are obtained from the isotherm data. In addition, the variation in phase morphology for the monolayer upon lateral compression is examined through *in situ* Brewster angle microscopy (BAM) and fluorescence microscopy (FM). Furthermore, topological observations were made using atomic force microscopy (AFM) of Langmuir-Blodgett (LB) films transferred onto a mica substrate.

2 EXPERIMENTAL

2.1 Materials

(Perfluorobutyl) undecanol (*F4H*11OH) was synthesized via the procedure reported previously[15]. L-α-dipalmitoylphosphatidylcholine (DPPC; purity > 99%) and the fluorescent probe 1-palmitoyl-2-[6-[(7-nitro-2-1,3-benzoxadiazol-4-yl) amino] hexanoyl]-*sn*-glycero-3-phosphocholine (NBD-PC) were obtained from Avanti Polar Lipids (Alabaster, AL). These lipids were used without further purification. Chloroform (99.7%) and methanol (99.8%) were used as spreading solvents and were obtained from Kanto Chemical Co., Inc (Tokyo, Japan) and nacalai tesque (Kyoto, Japan), respectively. The chloroform/methanol (2/1, v/v) mixtures were used as spreading solvents. Sodium chloride (nacalai tesque) was roasted at 1023 K for 24 h to remove all surface active organic impurities. The subphase solution was prepared using thrice distilled water (surface tension = 72.0 mN m^{-1} at 298.2 K; electrical resistivity = 18 MΩ cm).

2.2 Methods

Surface pressure-area isotherms

The surface pressure (π) of monolayers was measured using an automated custom-made Wilhelmy balance. The surface pressure balance (Mettler Toledo, AG-245) had a resolution of 0.01 mN m^{-1}. The pressure-measuring system was equipped with filter paper (Whatman 541, periphery = 4 cm). The trough was made from Teflon-coated brass (area = 720 cm^2). Teflon barriers (both hydrophobic and lipophobic) were used in this study. Surface pressure (π)-molecular area (*A*) isotherms were recorded at 298.2 ± 0.1 K. Stock solutions of DPPC (1.0 mM), and *F4H*11OH (1.0 mM) were prepared in chloroform/methanol (2/1, v/v). The spreading solvents were allowed to evaporate for 15 min prior to compression. The monolayer was compressed at a speed of ~0.10 nm^2 $molecule^{-1}min^{-1}$. The standard deviations (SD) for molecular surface area and surface pressure were ~0.01 nm^2 and ~0.1 mN m^{-1}, respectively[20,23,24].

Surface potential-area isotherms

The surface potential (ΔV) and surface pressure were recorded simultaneously when the monolayer was compressed and expanded at the air-water interface. The process was monitored using an ionizing ^{241}Am electrode, which was placed at 1-2 mm above the interface, while a reference electrode was dipped in the subphase. The electrometer (Keithley 614) was used to measure the surface potential. The SD for the surface potential was 5 mV[25,26].

Brewster angle microscopy (BAM)

The monolayer was directly visualized by a Brewster angle microscope (KSV Optrel BAM 300, KSV Instruments Ltd., Finland) coupled to a commercially available film balance system (KSV Minitrough, KSV Instruments Ltd.). Use of a 20 mW He-Ne laser emitting *p*-polarized light of 632.8 nm wavelength and a 10× objective lens allowed a lateral resolution of ~2 μm. The angle of the incident beam to the air-water interface was fixed to the Brewster angle (53.1°) at 298.2 K. The reflected beam was recorded with a high grade charge-coupled device (CCD) camera (EHDkamPro02, EHD Imaging GmbH, Germany), and the BAM images were digitally saved on the computer hard disk[24,27,28].

Fluorescence microscopy (FM)

The film balance system (KSV Minitrough) was mounted onto the stage of an Olympus microscope BX51WI (Tokyo, Japan) equipped with a 100 W mercury lamp (USH-1030L), an objective lens (SLMPlan50×, working distance = 15 mm), and a 3CCD camera with a camera control unit (IK-

TU51CU, Toshiba, Japan). A spreading solution of the co-solubilized samples was prepared and doped with 1 mol% of the fluorescence probe (NBD-PC). Image processing and analysis were carried out using Adobe Photoshop Elements ver. 7.0 (Adobe Systems Incorporated, CA) software. The total amount of ordered domains (dark contrast regions) was evaluated and expressed as a percentage per frame by dividing the respective frame into dark and bright regions. The resolution was 0.1% and the maximum SD was 8.9%. More details on FM measurements have been provided in a previous paper[12].

Atomic force microscopy (AFM)

Langmuir-Blodgett (LB) film preparations were carried out with the KSV Minitrough. Freshly cleaved mica (Okenshoji Co., Tokyo, Japan) was used as a supporting solid substrate for film deposition (vertical dipping method). At selected surface pressures, a transfer velocity of 5 mm min^{-1} was used for single-layer deposition. The film-forming materials were spread on 0.15 M NaCl at 298.2 K. The transfer occurs so that the hydrophilic part of the monolayer is in contact with mica while the hydrophobic part is exposed to air. LB films with a deposition rate of ~1 were used in the experiments. The AFM experiments were performed in the air at room temperature. The AFM images were obtained using an SPA 400 instrument (Seiko Instruments Co., Chiba, Japan) at room temperature in the tapping mode. This provided both topographical and phase contrast images. Other details about AFM measurements have been mentioned previously[23].

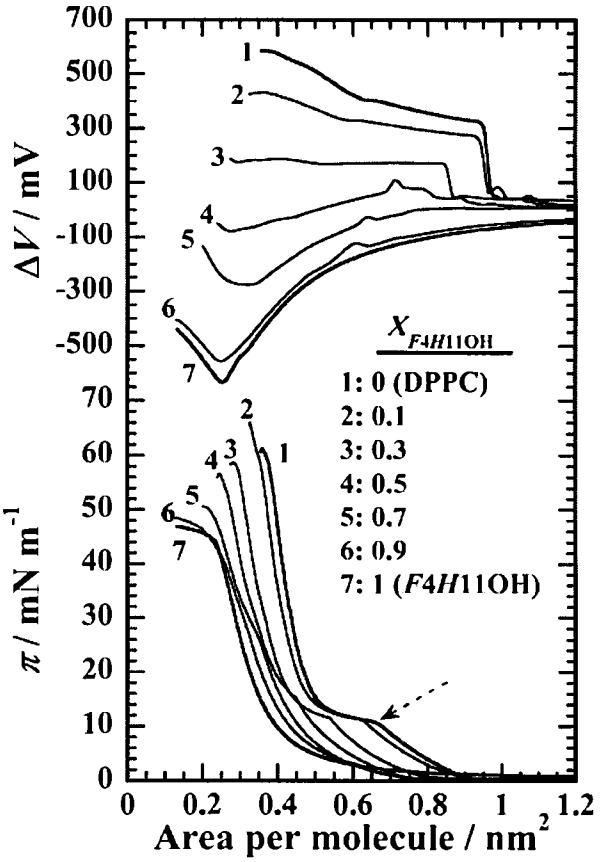

Fig. 1 The π-A and ΔV-A isotherms of the binary DPPC/*F4H*11OH monolayers on 0.15 M NaCl at 298.2 K.

3 RESULTS AND DISCUSSION

3.1 π-A and ΔV-A isotherms

*F4H*11OH monolayer stability at the air-water interface was checked by evaluating the temperature dependence of a phase transition pressure (π^{eq}) from disordered to ordered states and an apparent molar quantity change on phase transition, too[15]. The surface pressure (π)-molecular area (A) and surface potential (ΔV)-A isotherms for the two-component DPPC/*F4H*11OH systems on 0.15 M NaCl at 298.2 K are shown in Fig. 1. In the present condition, *F4H*11OH, which has a melting point of 308.6 K[15], should be in the solid state. *F4H*11OH forms a typical disordered monolayer at 298.2 K (*curve 7*). A collapse pressure (π^c) of *F4H*11OH monolayers is ~44 mN m^{-1} at 0.24 nm^2. The extrapolated area of highly packed states on the π-A isotherm is ~0.40 nm^2, which is based on the cross-sectional area of *F*-chains (~0.30 nm^2)[2]. DPPC monolayers (*curve 1*) have a liquid expanded (LE)/liquid condensed (LC) phase transition at ~11 mN m^{-1} (dashed arrow), which has been discussed previously[23, 29-31]. The π-A isotherms shift to smaller areas with increasing the mole fraction of *F4H*11OH ($X_{F4H11OH}$). The π^{eq} value increases as $X_{F4H11OH}$ increases, which means there is a fluidizing effect for *F4H*11OH on DPPC monolayers[24]. In the strict sense, the π^{eq} value is kept almost constant in the region of $0 \le X_{F4H11OH} \le 0.3$, although the increment in π^{eq} is apparently observed in $X_{F4H11OH} > 0.3$. This behavior is discussed in more detail in the latter section. The π^c value apparently changes with respect to $X_{F4H11OH}$, which suggests a miscibility between DPPC and *F4H*11OH in the monolayer state. The ΔV-A isotherms indicate completely different behavior between DPPC and *F4H*11OH monolayers. DPPC monolayers exhibit a positive increment in ΔV upon compression, whereas *F4H*11OH monolayers indicate a negative variation. As the monolayer orientation becomes more closely packed the values of ΔV increase by an order of magnitude. The negative ΔV value is strongly dependent on the terminal group (CF_3-) of *F4H*11OH and has been well-established[19, 24, 28]. The ΔV-A isotherms shift from positive to negative values for systems involving pure components as $X_{F4H11OH}$ increases. Similar variations for hydrocarbon-fluorocarbon systems have been reported previously[19, 20, 24].

3.2 Compressibility modulus

A compressibility modulus (or dilatational elasticity modulus, Cs^{-1}) is calculated from the π-A isotherm by the following equation:

$$Cs^{-1} = -A\left(\frac{\partial \pi}{\partial A}\right)_T \quad (1)$$

The $Cs^{-1}-\pi$ curve allows us to more readily determine the $\pi^{[9]}$ values and to elucidate the phase state of monolayers. For example, the curve for DPPC (see Fig. 2, *curve 1*) shows a more distinct kink (at ~11 mN m^{-1}) than is seen in the π-A isotherms (indicated by the dashed arrow), which corresponds to the transition. The kinks, which are indicated by dashed arrows, increase gradually with increasing $X_{F4H11OH}$ in Fig. 2. In addition, The Cs^{-1} values give information on the monolayer packing upon compression. It is well-known that a high compressibility modulus (or low compressibility) is a sign of tight packing and large cohesive forces between components of monolayers. According to the Davies and Rideal classification[32], values between 12.5 $<Cs^{-1}$ (in mN m^{-1}) <50 and $100<Cs^{-1}<250$ are evidence that the monolayer is in LE and LC states, respectively. Although the classification is defined for typical lipid monolayers, a previous study has described its validity for monolayers of fluorinated amphiphiles[16]. The maximum Cs^{-1} value decreases from ~225 (*curve 1*) to ~75 mN m^{-1} (*curve 4*) as $X_{F4H11OH}$ increases. This reduction supports the fluidization of DPPC monolayers by the *F4H*11OH addition.

3.3 Excess Gibbs free energy

The π-A isotherms for the binary DPPC/*F4H*11OH system (Fig. 1) can be also analyzed in terms of the excess Gibbs free energy of mixing (ΔG_{mix}^{exc}). The ΔG_{mix}^{exc} value is calculated from the following equation (Eq. (2))[33],

$$\Delta G_{mix}^{exc} = \int_0^{\pi} (A_{12} - X_1 A_1 - X_2 A_2)\, d\pi \quad (2)$$

where A_i and X_i are the molecular area and mole fraction of component i, respectively, and A_{12} is the mean molecular area in the binary monolayer. For identical interactions between the two components, the value of ΔG_{mix}^{exc} is zero, which means that they are ideally mixed in the monolayer[34, 35]. A negative deviation from ideality indicates an attractive interaction between the two components. The variations in ΔG_{mix}^{exc} for the DPPC/*F4H*11OH monolayer against $X_{F4H11OH}$ at typical surface pressures are shown in Fig. 3. In the range $0<X_{F4H11OH} \leq 0.7$, the values are nearly negative at all surface pressures. In addition, they decrease with an increase in $X_{F4H11OH}$. It is noted that the values at

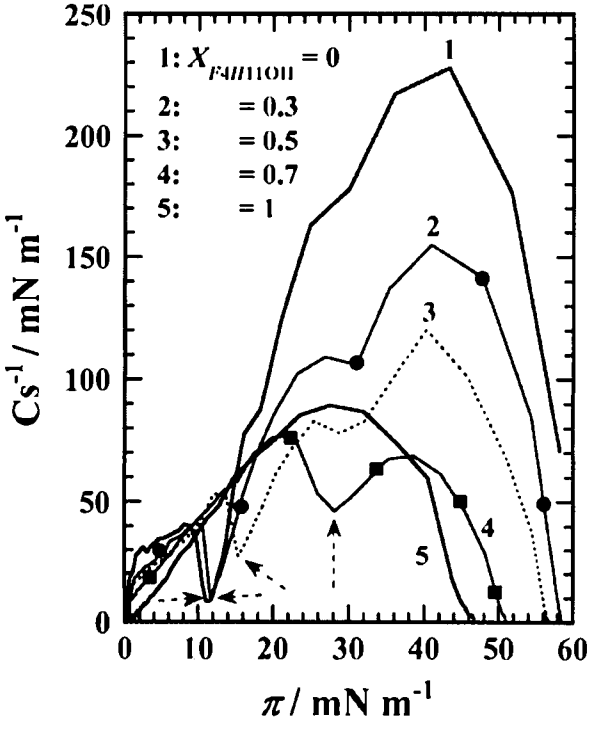

Fig. 2 Compressibility modulus (or dilatational elasticity modulus, Cs^{-1}) of the binary DPPC/*F4H*11OH monolayers as a function of π at typical molar fractions of *F4H*11OH ($X_{F4H11OH}$) on 0.15 M NaCl at 298.2 K.

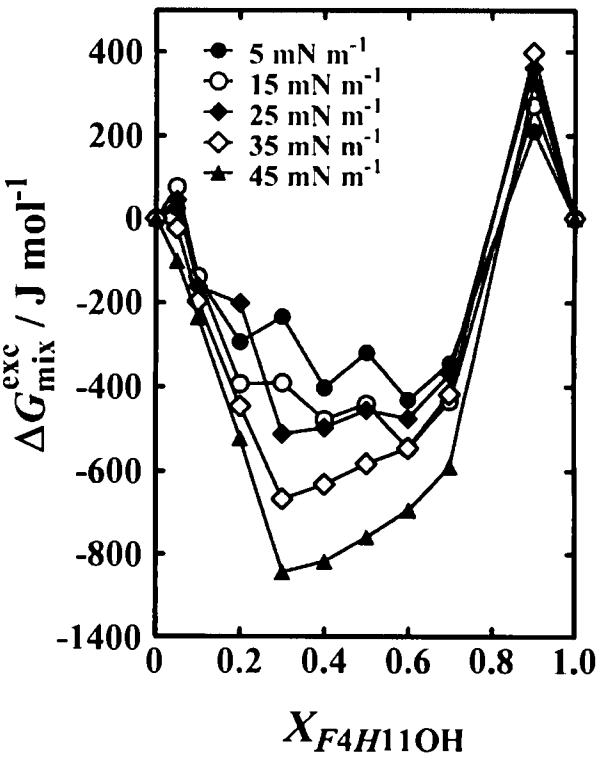

Fig. 3 Excess Gibbs free energy of mixing (ΔG_{mix}^{exc}) of the binary DPPC/*F4H*11OH monolayers as a function of $X_{F4H11OH}$ at typical surface pressures on 0.15 M NaCl at 298.2 K.

$X_{F4H11OH}=0.3$ reach approximately -850 J mol^{-1} as a minimum at 45 mN m^{-1}. This behavior suggests that the attractive force between hydrophobic chains of DPPC and *F4H*11OH increases upon compression and their affinity becomes largest at $X_{F4H11OH}=0.3$. On the other hand, at $X_{F4H11OH}=0.9$, ΔG_{mix}^{exc} exhibits positive values, which means that there is the existence of a repulsive force or a steric hindrance between the two components. This may be because a small amount of DPPC acts as a dye for *F4H*11OH[36-38]. Thus, the monolayer at $X_{F4H11OH}=0.9$ is considered to take a looser packing compared to an ideal mixing. Nevertheless, these results provide complementary evidence for the miscibility between them within a monolayer.

3.4 Two-dimensional phase diagrams

Figure 4 describes a two-dimensional (2-D) phase diagram for the binary system at 298.2 K, which is constructed by plotting the transition pressure (π^{eq}) and collapse pressure (π^{c}) values against $X_{F4H11OH}$. The π^{eq} values are kept almost constant below $X_{F4H11OH}=0.3$. However, they change positively as $X_{F4H11OH}$ increases from $X_{F4H11OH}=0.3$ to 0.7. In the high surface pressure region, the experimental π^{c} values vary against $X_{F4H11OH}$. Accordingly, the two components are found to be miscible in the monolayer state. The coexistence phase boundary between the monolayer phase (2-D) and bulk phase (3-D) of the molecules spread on the surface can be theoretically simulated from the Joos equation[39] under the assumption of a regular surface mixture,

$$1=x_1^s \exp\{(\pi_m^c-\pi_1^c)\omega_1/kT\} \exp\{\xi (x_2^s)^2\}$$
$$+x_2^s \exp\{(\pi_m^c-\pi_2^c)\omega_2/kT\} \exp\{\xi (x_1^s)^2\} \quad (3)$$

where x_1^s and x_2^s denote the respective mole fractions in the two-component monolayer consisting of components 1 and 2; π_1^c and π_2^c are the respective collapse pressures of components 1 and 2 and π_m^c is the collapse pressure of the binary monolayer at a given composition of x_1^s (or x_2^s); ω_1 and ω_2 are the corresponding molecular areas at collapse; ξ is the interaction parameter; and kT is the product of the Boltzmann constant and the Kelvin temperature. The solid curve at higher surface pressures was obtained by adjusting the interaction parameter in Eq. (3) to achieve the best fit for the experimental values of collapse pressures. As a result, the phase diagram for the binary system is a positive azeotropic type. It is noteworthy that the binary system exhibits negative interaction parameters and has two different interaction behavior in the two regions: $\xi=-1.57$ for $0<X_{F4H11OH}\leq 0.4$ and $\xi=-0.44$ for $0.4\leq X_{F4H11OH}\leq 1$. In particular, the monolayer for the latter is in almost the same as it would be in the ideal mixing state.

The interaction energy ($\Delta\varepsilon$) is given as follows:

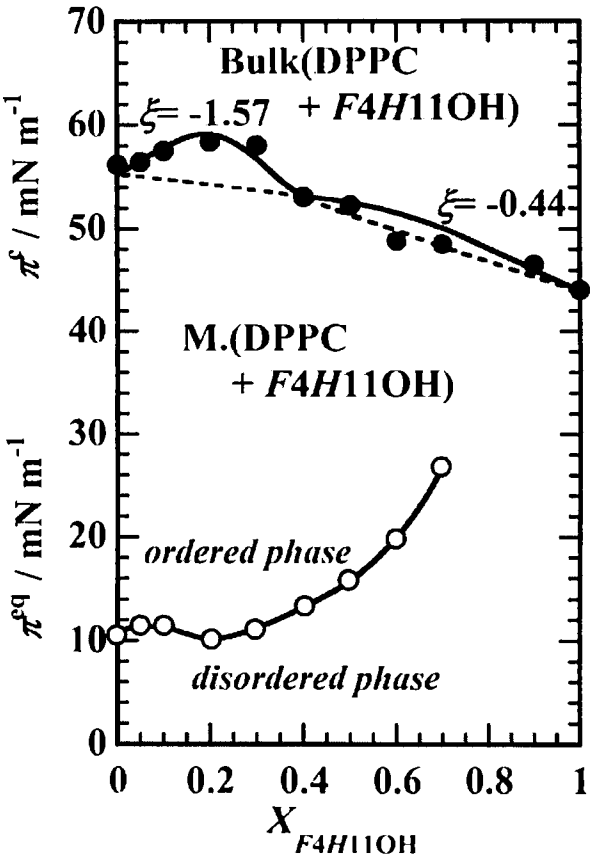

Fig. 4 Two-dimensional phase diagrams based on the variation of the transition pressure (π^{eq}: open circle) and collapse pressure (π^{c}: solid circle) on 0.15 M NaCl at 298.2 K as a function of $X_{F4H11OH}$. The dashed lines were calculated according to Eq. (3) for $\xi = 0$. The solid line at high surface pressures was obtained by curve fitting of experimental collapse pressures to Eq. (3). M. indicates a mixed monolayer formed by the lipids and *F4H*11OH species, whereas Bulk denotes a solid phase of the lipids and *F4H*11OH ("bulk phase" may be called "solid phase").

$$\Delta\varepsilon=\xi RT/z, \quad (4)$$

where z is the number of nearest neighbors, equal to 6, in a close-packed monolayer and the interaction energy is $\Delta\varepsilon=\varepsilon_{12}-(\varepsilon_{11}+\varepsilon_{22})/2$[39]; ε_{ij} denotes the potential energy of interaction between components i and j. The calculated interaction energies were -649 J mol^{-1} ($\xi=-1.57$) and -182 J mol^{-1} ($\xi=-0.44$). That is, the two components are miscible within a monolayer, since the interaction energies between them are smaller than $2RT$ (4958.7 J mol^{-1}).

An interaction mode at low surface pressures is entirely different from that found at high surface pressures. In $0\leq$

$X_{F4H11OH} \leq 0.3$, the two components do not interact favorably because of the almost constant π^{eq} value, as seen against $X_{F4H11OH}$. Considering the negative ξ value, however, it is found that *F4H*11OH interacts strongly with DPPC monolayers at high surface pressures. On the other hand, the opposite behavior is observed in $0.3 \leq X_{F4H11OH} \leq 1$. In this case, the addition of *F4H*11OH induces the fluidization of DPPC monolayers at low surface pressures and exerts few interactive influences on them at high surface pressures. This is not the general case in the situation where the interaction mode at low surface pressures is similar to that at high surface pressures for the binary systems of hydrocarbon/hydrocarbon[40, 41] and hydrocarbon/perfluorocarbon (including partially fluorocarbone)[19, 24, 28]. Judging from the fact that the DPPC/*F8H*11OH system applies to the first case[28], the phenomenon in the present study may occur because of the compact corn-swing motion of the perfluorobutyl moiety in *F4H*11OH at the fulcrum in the CH_2-CF_2 linkage. In comparison to the DPPC/*F8H*11OH system, the interaction parameter for the DPPC/*F4H*11OH system is considerably smaller in the DPPC-rich region[28]. The addition of *F8H*11OH causes solidification of the DPPC monolayers, which is not observed for the *F4H*11OH system. That is, the difference in the hydrophobic chain length by 4 perfluorinated methylene groups produces the inverse effect on DPPC monolayers. This points to the possibility that low fluorination in a molecule may lead to unique and drastic changes in its physical and chemical properties.

3.5 *In situ* BAM observations

The phase behavior of the binary DPPC/*F4H*11OH monolayer upon lateral compression has been morphologically elucidated with Brewster angle microscopy (BAM). Shown in Fig. 5 are the BAM images for the binary system at $X_{F4H11OH} = 0$ (DPPC), 0.1, 0.3, and 0.4. These BAM images indicate a coexistent state of disordered (dark contrast) and ordered (bright contrast) phases. DPPC monolayers

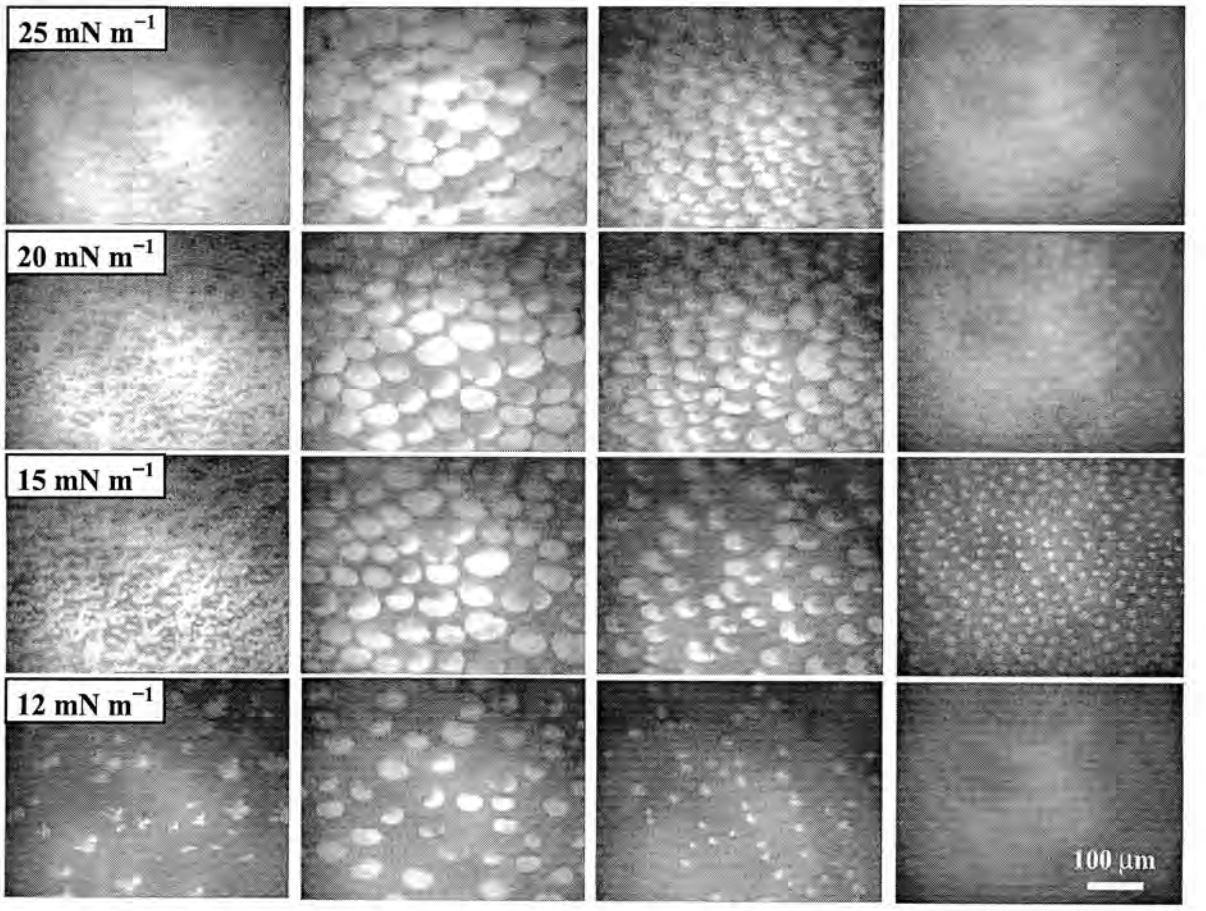

Fig. 5 BAM images of the binary DPPC/*F4H*11OH monolayers for $X_{F4H11OH}$ = 0 (DPPC), 0.1, 0.3, and 0.4 at 12, 15, 20, and 25 mN m^{-1} on 0.15 M NaCl at 298.2 K. The scale bar in the lower right represents 100 μm.

below the transition pressure ($\pi^{eq} = \sim 11$ mN m^{-1}) produce a homogeneously dark image (data not shown). With the monolayer compression above the pressure, LC domains are formed and then become larger in size and number. Finally, the image becomes optically bright above 25 mN m^{-1} [12,28]. It is widely accepted that a domain formation is controlled by the balance of line tension at the boundary between the disordered and ordered domains and long-range dipole-dipole interactions between the ordered domains. In the images at $X_{F4H11OH} = 0.1$, the addition of *F4H*11OH induces an increment in ordered domain size. Furthermore, the domain shape changes to a round form. This means that the addition of a small amount of *F4H*11OH enhances the contribution of the line tension at the phase boundary. However, further addition induces a size reduction in ordered domains at $X_{F4H11OH} = 0.3$ and 0.4. These phenomena correspond to the fluidizing effect on DPPC monolayers[24]. It is worthwhile that at $X_{F4H11OH} = 0.4$, ordered domains dissolve into disordered domains with increasing surface pressures from 15 to 20 mN m^{-1}. However, the specific behavior is not as easily observed from the BAM image due to the relatively low magnification and resolution of the apparatus. More detailed morphological observations are discussed in the next section.

3.6 *In situ* FM observations

Figure 6 shows the *in situ* FM images for the DPPC/*F4H*11OH monolayer at the air-water interface. Bright and dark contrasts in the FM image respectively correspond to disordered and ordered phases as opposed to the corresponding BAM image. In the FM observation, the binary monolayer contains a small amount of a fluorescent probe (1 mol% NBD-PC). There is a possibility that the introduction of the probe may change the original phase behavior of the monolayer. However, similarity between the BAM (Fig. 5) and FM (Fig. 6) images would indicate that this is

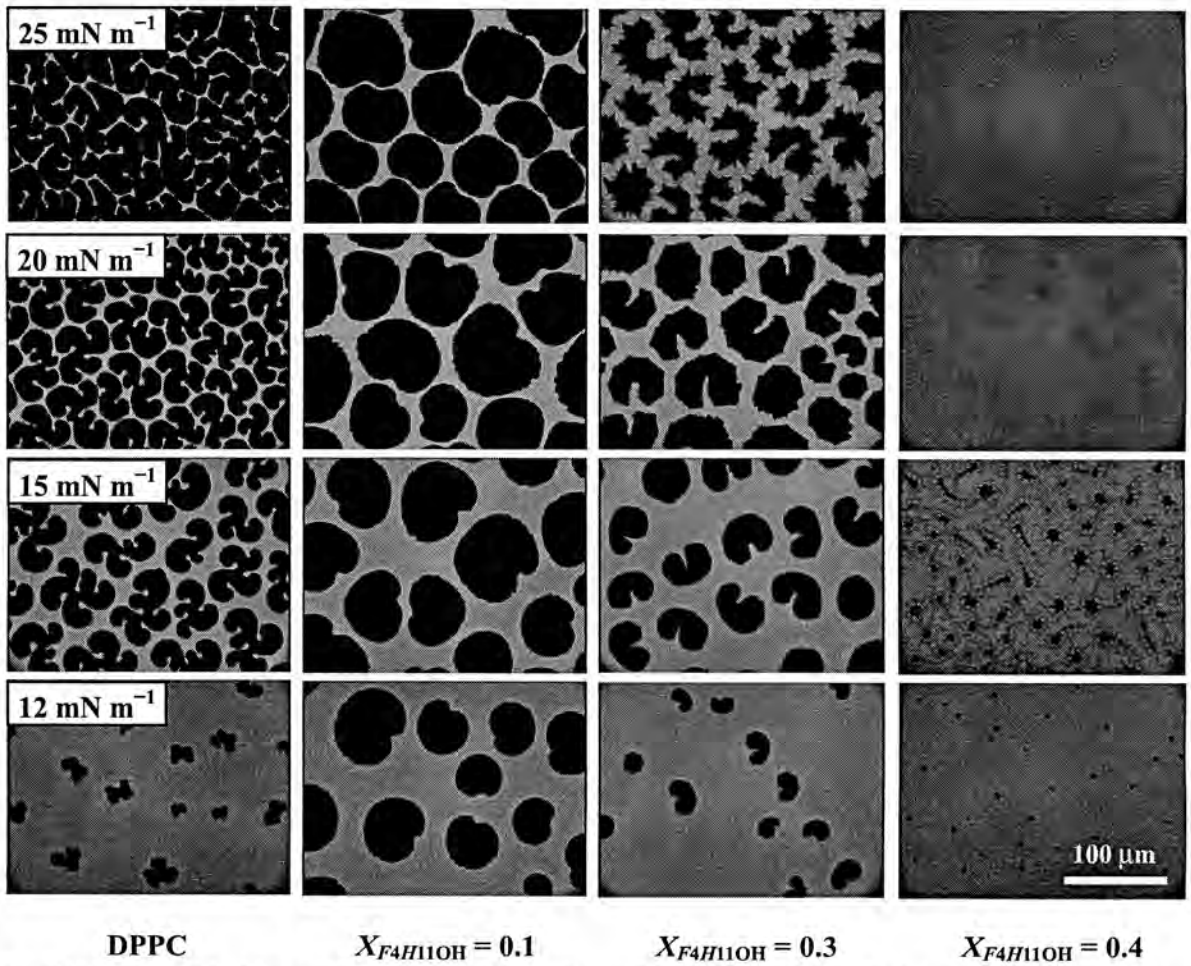

Fig. 6 FM images of the binary DPPC/*F4H*11OH monolayers for $X_{F4H11OH} = 0$ (DPPC), 0.1, 0.3, and 0.4 at 12, 15, 20, and 25 mN m^{-1} on 0.15 M NaCl at 298.2 K. The monolayers contain 1 mol% of fluorescent probe (NBD-PC). The scale bar in the lower right represents 100 μm.

not the case. Generally, FM observations generate a picture with higher resolution, magnification, and contrast compared to BAM observations. As for the DPPC monolayer, the images exhibit LC domains that are coexistent with LE regions in a clear and sharp contrast. As $X_{F4H11OH}$ increases, the size and appearance of ordered domains vary similarly to the corresponding BAM image (Fig. 5). It is noted that the dissolution phenomenon mentioned in the previous section is clearly seen at $X_{F4H11OH} = 0.4$ (15 mN m^{-1}). At the image, there are three kinds of domains; disordered domains, ordered domains, and domains (gray contrast) that represent an intermediate state between disordered and ordered domains. The ordered domain is transformed through the intermediate state into disordered states by further compression to 20 mN m^{-1}. Interestingly, the specific transfer occurs at a phase boundary between disordered and ordered domains or an edge of the ordered domains. The same behavior is also observed at $X_{F4H11OH} = 0.3$ (25 mN m^{-1}). This phenomenon clearly indicates a surface-pressure-induced fluidizing effect of *F4H11OH* on DPPC monolayers. Although there are many papers on the fluidizing effect induced by surface compositions[24, 30, 42, 43], to our knowledge, a surface-pressure-induced fluidizing effect is reported here for the first time. In addition, the observed effect is consistent with the π^{eq} behavior in the phase diagram (Fig. 4); the onset of the increment in π^{eq} is reflected in the surface-pressure-induced effect, which is also evident in BAM and FM observations. Apparently, the present system exerts not only a surface-pressure-induced effect (morphologically) but also a surface-composition-induced effect (thermodynamically). A percentage of the ordered domain per frame of FM images is plotted as a function of surface pressure in Fig. 7. In the range $0 \leq X_{F4H11OH} \leq 0.2$, the ordered domain ratio increases monotonically and finally approaches ~95% upon compression. Thus, it is found that the addition of a small-amount of *F4H11OH* ($0 \leq X_{F4H11OH} \leq 0.2$) does not induce the fluidizing effect. This behavior agrees well with the results seen in Fig. 4. However, the percentage at $X_{F4H11OH} = 0.3$ and 0.4 does not reach the value. On the contrary, a sudden reduction in percentage during increasing surface pressures within ~5 mN m^{-1} is caused after 22 ($X_{F4H11OH} = 0.3$) and 14 mN m^{-1} ($X_{F4H11OH} = 0.4$). Considering the fact that the fluidizing effect induced by surface pressures is not observed for the binary DPPC/*F8H5OH*[24] and DPPC/*F8H11OH* systems[28], it is speculated that the compact corn-swing motion of the perfluorobutyl moiety in *F4H11OH* at the fulcrum in the CH_2-CF_2 linkage disturbs the ordered domain at the phase boundary or from its edge upon compression.

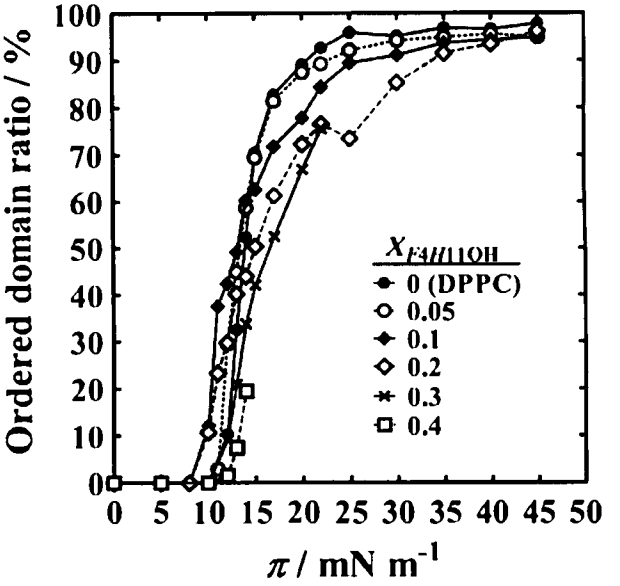

Fig. 7 Surface-pressure dependence of the ratio of ordered domain (dark contrast) area in FM images of the binary DPPC/*F4H11OH* monolayers for $X_{F4H11OH}$ = 0, 0.05, 0.1, 0.2, 0.3, and 0.4.

3.7 AFM topographical observation

The phase behavior of the binary DPPC/*F4H11OH* system has been visualized *in situ* at the air-water interface with FM and BAM on the micrometer scale. Unfortunately, such observations could not clarify the phase morphology in the range $0.4 < X_{F4H11OH} < 1$ because of the limited optical resolution and magnification of the microscopes. Higher $X_{F4H11OH}$ ranges are of significant value for elucidating the binary miscibility. Therefore, the morphology of LB films transferred onto a mica at $X_{F4H11OH} = 0.5$, 0.7, and 0.9 has been characterized by AFM (Fig. 8). The AFM topographies for pure DPPC and *F4H11OH* monolayers at 35 mN m^{-1} are optically homogeneous (data not shown). The AFM images at $X_{F4H11OH} = 0.5$ show many string-like fragments (bright contrast) composed almost completely of DPPC. The height difference between the fragment and the surrounding network (dark contrast), which composed almost completely of *F4H11OH*, is observed to be ~0.5 nm irrespective of the increase in surface pressure from 20 to 35 mN m^{-1}. This means that *F4H11OH* reclines against the DPPC monolayers owing to the similarity of the hydrophobic chain lengths between them. Considering the surface-pressure-induced fluidizing effect, the fragments are thought to be a product that is generated by the fluidizing effect of *F4H11OH*. On increasing $X_{F4H11OH}$ to 0.7 and 0.9, the AFM images exhibit homogeneous, flat topologies, which indicates the miscibility between DPPC and *F4H11OH* on the nanometer scale.

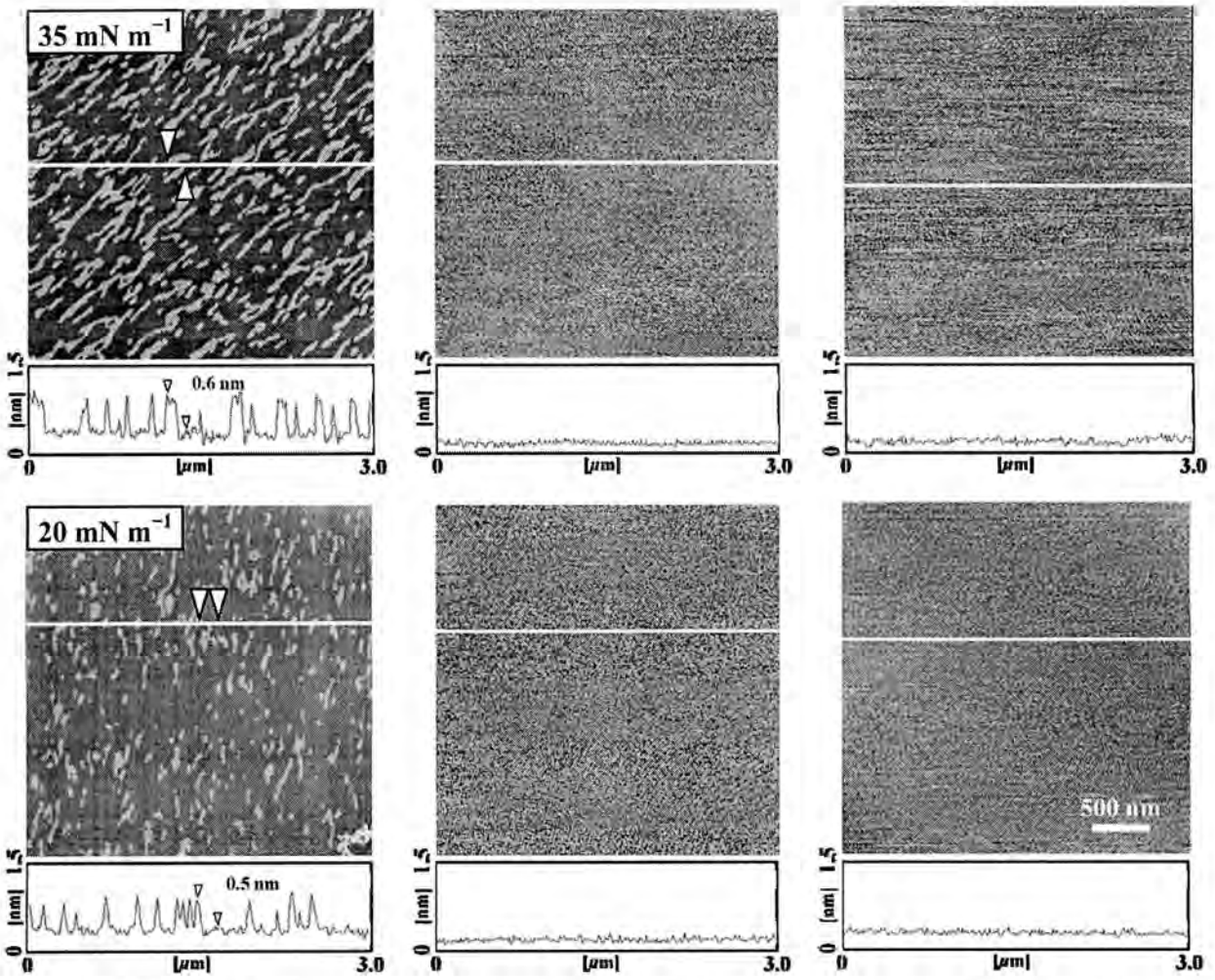

Fig. 8 Typical AFM topographic images of the binary DPPC/*F4H*11OH systems for $X_{F4H11OH}$ = 0.5, 0.7, and 0.9 at 20 and 35 mN m^{-1}. The scan area is 3.0 × 3.0 μm. The cross-sectional profiles along the scanning line (white line) are given just below the respective AFM images. The height difference between the arrows is indicated in the cross-sectional profile.

4 CONCLUSION

*F4H*11OH is miscible with DPPC in the monolayer state from both thermodynamic and morphological perspectives. The 2-D phase diagrams were constructed by plotting the surface pressure of phase transitions from disordered to ordered states and of monolayer collapsing against $X_{F4H11OH}$. The binary monolayer exists as the positive azeotrope type in the π^c region of the phase diagram. The interaction parameter and interaction energy were evaluated under the assumption of a regular surface mixture. In addition, the excess Gibbs free energy of mixing for the present system was calculated on the basis of the additivity rule. The energy indicates that *F4H*11OH interacts attractively with DPPC and the interaction mode is most stable at $X_{F4H11OH}$ = 0.3. Morphological observations with BAM, FM, and AFM also support the monolayer miscibility for the system on the micro- and nanometer scales. Furthermore, these observations suggest the following conclusions: the fluidizing effect on DPPC monolayers is not observed on adding a small amount of *F4H*11OH ($0 \leq X_{F4H11OH} \leq 0.2$) and but is only observed with the addition of a moderate amount ($0.3 \leq X_{F4H11OH} \leq 0.5$). Furthermore, it is noted that in the latter case, the fluidizing effect is induced by surface pressures and not by surface composition. The emergence of this specific effect is considered to be based on the balance between the lengths of *H*-chains and *F*-chains in a molecule. This understanding of the surface-induced fluidizing effect on DPPC monolayers should be helpful for designing

an additive to pulmonary surfactants.

5 ACKNOWLEDGEMENTS

This work was supported by a Grant-in-Aid for Scientific Research 23510134 from the Japan Society for the Promotion of Science (JSPS). It was also supported by a Grant-in-Aid for Young Scientists (B) 22710106 from JSPS and by a Foundation from Oil & Fat Industry Kaikan (H.N.).

References

1) Kissa, E., *Fluorinated Surfactants and Repellents. 2nd ed., revised and expanded.* Surfactant Science Series 97; Hubbard, A. T., Ed.; Marcel Dekker Inc.: Basel, New York, pp 1-615 (2001).
2) Riess, J. G. Fluorous micro- and nanophases with a biomedical perspective. *Tetrahedron* 58, 4113-4131 (2002).
3) Krafft, M. P. Fluorocarbons and fluorinated amphiphiles in drug delivery and biomedical research. *Adv. Drug Deliv. Rev.* 47, 209-228 (2001).
4) Riess, J. G. Oxygen carriers ("blood substitutes")-raison d'etre, chemistry, and some physiology. *Chem. Rev.* 101, 2797-2920 (2001).
5) Higgins, C. P.; Luthy, R. G. Sorption of perfluorinated surfactants on sediments. *Environ. Sci. Technol.* 40, 7251-7256 (2006).
6) Burns, D. C.; Ellis, D. A.; Li, H.; McMurdo, C. J.; Webster, E. Experimental pKa determination for perfluorooctanoic acid (PFOA) and the potential impact of pKa concentration dependence on laboratory-measured partitioning phenomena and environmental modeling. *Environ. Sci. Technol.* 42, 9283-9288 (2008).
7) Goss, K. U. The pKa values of PFOA and other highly fluorinated carboxylic acids. *Environ. Sci. Technol.* 42, 456-458 (2008).
8) Riess, J. G. Highly fluorinated amphiphilic molecules and self-assemblies with biomedical potential. *Curr. Opin. Colloid Interf. Sci.* 14, 294-304 (2009).
9) Nakahara, H.; Shibata, O. Langmuir monolayer miscibility of perfluorocarboxylic acids with biomembrane constituents at the air-water interface. *J. Oleo Sci.* 61, 197-210 (2012).
10) Riess, J. G. Understanding the fundamentals of perfluorocarbons and perfluorocarbon emulsions relevant to in vivo oxygen delivery. *Artif. Cells Blood Subst. Immobil. Biotechnol.* 33, 47-63 (2005).
11) Riess, J. G. Perfluorocarbon-based oxygen delivery. *Artif. Cells Blood Subst. Immobil. Biotechnol.* 34, 567-580 (2006).
12) Nakahara, H.; Lee, S.; Krafft, M. P.; Shibata, O. Fluorocarbon-hybrid pulmonary surfactants for replacement therapy-a Langmuir monolayer study. *Langmuir* 26, 18256-18265 (2010).
13) Broniatowski, M.; Dynarowicz-Latka, P. Semifluorinated alcohols in Langmuir monolayers-a comparative study. *J. Colloid Interface Sci.* 301, 315-322 (2006).
14) Krafft, M. P.; Riess, J. G. Perfluorocarbons: Life Sciences and Biomedical Uses. *J. Polym. Sci. Part A: Polymer Chem.* 45, 1185-1198 (2007).
15) Nakahara, H.; Nakamura, S.; Okahashi, Y.; Kitaguchi, D.; Kawabata, N.; Sakamoto, S.; Shibata, O. Examination of fluorination effect on physical properties of saturated long-chain alcohols by DSC and Langmuir monolayer. *Colloids Surf. B* 102, 472-478 (2013).
16) Lehmler, H.-J.; Oyewumi, M. O.; Jay, M.; Bummer, P. M. Behavior of partially fluorinated carboxylic acids at the air-water interface. *J. Fluorine Chem.* 107, 141-146 (2001).
17) Krafft, M. P., *Highly fluorinated Langmuir-Blodgett and Gibbs monolayers.* Advanced Chemistry of Monolayers at Interfaces Imae, T., Ed.; Elsevier: Amsterdam, pp 177-191 (2007).
18) Krafft, M. P.; Riess, J. G. Chemistry, physical chemistry, and uses of molecular fluorocarbon-hydrocarbon diblocks, triblocks, and related compounds--unique "apolar" components for self-assembled colloid and interface engineering. *Chem. Rev.* 109, 1714-1792 (2009).
19) Nakahara, H.; Nakamura, S.; Kawasaki, H.; Shibata, O. Properties of two-component Langmuir monolayer of single chain perfluorinated carboxylic acids with dipalmitoylphosphatidylcholine (DPPC). *Colloids Surf. B* 41, 285-298 (2005).
20) Nakahara, H.; Tsuji, M.; Sato, Y.; Krafft, M. P.; Shibata, O. Langmuir monolayer miscibility of single-chain partially fluorinated amphiphiles with tetradecanoic acid. *J. Colloid Interf. Sci.* 337, 201-210 (2009).
21) Yokoyama, H.; Nakahara, H.; Shibata, O. Miscibility and phase behavior of DPPG and perfluorocarboxylic acids at the air-water interface. *Chem. Phys. Lipids* 161, 103-114 (2009).
22) Rontu, N.; Vaida, V. Miscibility of perfluorododecanoic acid with organic acids at the air-water interface. *J. Phys. Chem. C* 111, 9975-9980 (2007).
23) Nakahara, H.; Lee, S.; Sugihara, G.; Shibata, O. Mode of interaction of hydrophobic amphiphilic α-helical peptide/dipalmitoylphosphatidylcholine with phosphatidylglycerol or palmitic acid at the air-water interface. *Langmuir* 22, 5792-5803 (2006).
24) Nakamura, S.; Nakahara, H.; Krafft, M. P.; Shibata, O. Two-component Langmuir monolayers of single-chain partially fluorinated amphiphiles with dipalmitoylphosphatidylcholine (DPPC). *Langmuir* 23, 12634-12644

(2007).
25) Nakahara, H.; Shibata, O.; Moroi, Y. Examination of surface adsorption of sodium chloride and sodium dodecyl sulfate by surface potential measurement at the air/solution interface. *Langmuir* 21, 9020-9022 (2005).
26) Nakahara, H.; Shibata, O.; Rusdi, M.; Moroi, Y. Examination of Surface Adsorption of Soluble Surfactants by Surface Potential Measurement at the Air/Solution Interface. *J. Phys. Chem. C* 112, 6398-6403 (2008).
27) Matsumoto, Y.; Nakahara, H.; Moroi, Y.; Shibata, O. Langmuir monolayer properties of perfluorinated double long-chain salts with divalent counterions of separate electric charge at the air-water interface. *Langmuir* 23, 9629-9640 (2007).
28) Nakahara, H.; Krafft, M. P.; Shibata, A.; Shibata, O. Interaction of a partially fluorinated alcohol (*F8H11OH*) with biomembrane constituents in two-component monolayers. *Soft Matter* 7, 7325-7333 (2011).
29) Nakahara, H.; Lee, S.; Shibata, O. Pulmonary surfactant model systems catch the specific interaction of an amphiphilic peptide with anionic phospholipid. *Biophys. J.* 96, 1415-1429 (2009).
30) Hiranita, T.; Nakamura, S.; Kawachi, M.; Courrier, H. M.; Vandamme, T. F.; Krafft, M. P.; Shibata, O. Miscibility behavior of dipalmitoylphosphatidylcholine with a single-chain partially fluorinated amphiphile in Langmuir monolayers. *J. Colloid Interf. Sci.* 265, 83-92 (2003).
31) Hoda, K.; Nakahara, H.; Nakamura, S.; Nagadome, S.; Sugihara, G.; Yoshino, N.; Shibata, O. Langmuir monolayer properties of the fluorinated-hydrogenated hybrid amphiphiles with dipalmitoylphosphatidylcholine (DPPC). *Colloids Surf. B* 47, 165-175 (2006).
32) Davies, J. T.; Rideal, E. K., *Interfacial Phenomena*. 2nd ed.; Ed.; Academic Press: New York, pp 480 (1963).
33) Goodrich, F. C. In *Proceeding of 2nd International Congress on Surface Activity*, J. H. Schulman ed., London, 1957; Butterworth & Co.: London, 1957; p 85.
34) Marsden, J.; Schulman, J. H. *Trans. Faraday Soc.* 34, 748-758 (1938).
35) Shah, D. O.; Schulman, J. H. *J. Lipid Res.* 8, 215-226 (1967).
36) Weis, M.; Vančo, M.; Vitovič, P.; Hianik, T.; Cirák, J. Study of Gramicidin A-phospholipid interactions in Langmuir monolayers: analysis of their mechanical, thermodynamical, and electrical properties. *J. Phys. Chem. B* 110, 26272-26278 (2006).
37) Hąc-Wydro, K.; Kapusta, J.; Jagoda, A.; Wydro, P.; Dynarowicz-Łątka, P. The influence of phospholipid structure on the interactions with nystatin, a polyene antifungal antibiotic A Langmuir monolayer study. *Chem. Phys. Lipids* 150, 125-135 (2007).
38) Nagadome, S.; Suzuki, N. S.; Mine, Y.; Yamaguchi, T.; Nakahara, H.; Shibata, O.; Chang, C. H.; Sugihara, G. Monolayers (Langmuir films) behavior of multi-component systems composed of a bile acid with different sterols and with their 1:1 mixtures. *Colloids Surf. B* 58, 121-136 (2007).
39) Joos, P.; Demel, R. A. The interaction energies of cholesterol and lecithin in spread mixed monolayers at the air-water interface. *Biochim. Biophys. Acta* 183, 447-457 (1969).
40) Nakahara, H.; Nakamura, S.; Nakamura, K.; Inagaki, M.; Aso, M.; Higuchi, R.; Shibata, O. Cerebroside Langmuir monolayers originated from the echinoderms I. Binary systems of cerebrosides and phospholipids. *Colloids Surf. B* 42, 157-174 (2005).
41) Hoda, K.; Ikeda, Y.; Kawasaki, H.; Yamada, K.; Higuchi, R.; Shibata, O. Mode of interaction of ganglioside Langmuir monolayer originated from echinoderms: three binary systems of ganglioside/DPPC, ganglioside/DMPE, and ganglioside/cholesterol. *Colloids Surf. B* 52, 57-75 (2006).
42) Lehmler, H.-J.; Jay, M.; Bummer, P. M. Mixing of Partially Fluorinated Carboxylic Acids and Their Hydrocarbon Analogues with Dipalmitoylphosphatidylcholine at the Air-Water Interface. *Langmuir* 16, 10161-10166 (2000).
43) Lehmler, H.-J.; Bummer, P. M. Mixing behavior of 10-(perfluorohexyl)-decanol and DPPC. *Colloids Surf. B* 44, 74-81 (2005).